SUPLEMENTARY INFORMATION

Induction of multiple myeloma bone marrow stromal cell apoptosis by inhibiting extracellular vesicle *miR-10a* secretion

Tomohiro Umezu[1,2,*], Satoshi Imanishi[3], Seiichiro Yoshizawa[1], Chiaki Kawana[1], Junko H. Ohyashiki[2], and Kazuma Ohyashiki[1,2]

[1]Department of Hematology, Tokyo Medical University, Tokyo, Japan

[2]Department of Advanced Cellular Therapy, Tokyo Medical University, Tokyo, Japan

[3]Institute of Medical Science, Tokyo Medical University, Tokyo, Japan

Current address of TU is Department of Molecular Pathology, Tokyo Medical University, Tokyo, Japan.

*Correspondence: Tomohiro Umezu, Tokyo Medical University, 6-7-1 Nishi-shinjuku, Shinjuku, Tokyo 160-0023, Japan.

Tel: +81-3-3342-6111; Fax: +81-3-3345-0185; E-mail: t_umezu@tokoy-med.ac.jp

SUPPLEMENTARY METHODS

Isolation of MM-BMSCs. bone marrow aspirate samples were obtained from MM patients and stromal cell cultures were generated from the adherent fraction cultured in mesenchymal stem cell basal medium (MSCBM) with SingleQuots kit (MSCGM; Lonza, Basel, Switzerland) medium supplemented with 10% heat-inactivated fetal bovine serum (HyClone, Thermo Fisher Scientific, Waltham, MA, USA), 100 IU/ml penicillin, and 100 μg/ml streptomycin (Gibco, Invitrogen, Carlsbad, CA, USA).

SA-β-gal staining. BMSCs were fixed in 0.2% glutaraldehyde, washed with phosphate-buffered saline (PBS), and incubated overnight at 37°C (without CO_2) with staining solution (1 mg/ml X-gal in 40 mM citric acid/sodium phosphate, pH 6.0, 5 mM potassium ferrocyanide, 5 mM potassium ferricyanide, 150 mM NaCl, and 2 mM $MgCl_2$). After incubation, the cells were washed with PBS and imaged for the presence of blue color.

Flow cytometry analysis. MM-BMSCs were characterized by immunostaining of their surface antigens using the following monoclonal antibodies: CD90-FITC, CD73-allophycocyanin,

CD105-PerCPCy5.5, CD34-FITC, CD45-phycoerythrin, and HLA-DR-PreCPCy5.5 (BD Bioscience, San Jose, CA, USA). The BMSCs were stained and analyzed using an Accuri C6 cytometer (BD Bioscience) according to the manufacturer's instructions.

Detection of cell viability and apoptosis. Apoptosis was also detected using an FITC Annexin V Apoptosis Detection Kit I (BD Bioscience). Cells treated with exosome inhibitor (FTY720 or GW4869) or miR-10a mimic were suspended in binding buffer and incubated with FITC-labeled annexin V and PI in the dark, and then analyzed using an Accuri C6 cytometer (BD Bioscience) according to the manufacturer's instructions.

Nanoparticle tracking analysis of extracellular vesicles (EVs). Nanoparticle tracking analysis (NTA) measurements were performed using a Nanosight LM10 system (Malvern, Herrenberg, Germany) equipped with a blue laser (405 nm). Exosomes were illuminated by the laser and their movement under Brownian motion was recorded in 90-s sample videos, which were analyzed with NTA 2.0 analytical software (Malvern). All samples were serially diluted with phosphate-buffered saline (PBS) to obtain particle concentrations suitable for NTA (1×10^8 to

2.5 × 10^9 particles/ml). The capture settings (shutter and gain) and analysis settings were performed manually according to the manufacturer's instructions. All analysis settings were kept uniform between experiments. NTAs were averaged within each sample across the video replicates and then averaged across samples to determine total nanoparticle concentrations. The nanoparticle concentrations were normalized to the number of cells at the time of harvest.

Transmission electron microscopy. For analysis by transmission electron microscopy, exosomes were prepared, fixed with 4% paraformaldehyde and 4% glutaraldehyde in 0.1 M phosphate buffer (pH 7.4) at room temperature, and placed in a refrigerator to lower the temperature of the samples to 4°C. The samples were adsorbed to a 400-mesh carbon-coated grid and immersed in 2% phosphor tungstic acid solution (pH 7.0) for 30 s. The samples were then observed with a transmission electron microscope (JEM-1200EX; JEOL Ltd., Japan) at an acceleration voltage of 80 kV.

miRNA expression profiles. Cellular and EV fractions were dissolved in 700 µl of QIAzol lysis reagent (Qiagen, Valencia, CA, USA). After incubation for 2 min, 1 µl of 1 nM

ath-miR-159 (Hokkaido System Science, Hokkaido, Japan) was added to each aliquot as a spike control for losses in preparation, followed by vortexing for 30 s and incubation on ice for 10 min. Subsequent cartridge filtration was performed according to the manufacturer's instructions. miRNA profiling of both cells and exosomes was performed using a TaqMan low-density miRNA array (Applied Biosystems, Carlsbad, CA, USA) according to the manufacturer's recommendations. RNU6B was used as an invariant control for cellular miRNA. The synthetic spike control (ath-miR-159) was used as an invariant control for EV miRNA. TaqMan miRNA assays (Applied Biosystems) were used to identify the individual miRNAs using SDS2.2 software (Applied Biosystems). Cell and EV samples were analyzed in duplicate and standardized to RNU6B and ath-miR-159, respectively.

Microarray experiment. Total RNA derived from bone marrow stromal cells (BMSCs) and multiple myeloma (MM) cell lines (RPMI8226, KMS-11, U266) was prepared with QIAzol Reagent (Qiagen). The quality of the extracted RNA was assessed using an Agilent Bioanalyzer (Agilent Technologies). Three hundred nanograms of total RNA from each sample was processed for hybridization onto a GeneChip® Human Gene 2.0 ST Array (Affymetrix, Santa

Clara, CA, USA) according to the manufacturer's protocol, and scanned. Raw and normalized data have been submitted to GEO and are available under series GSE108915 and GSE118282.

Direct transfection of miRNA mimics into EVs. The miRNA mimics or miRNA inhibitor (Ambion, Invitrogen) were labeled with a Label IT siRNA Tracker Cy3 kit (Mirus, Madison, WI, USA) according to the manufacturer's instructions. EVs derived from BMSCs (4×10^7 particles) were combined with 20 pmol Cy3-labeled miR-10a mimic and 10 μl Exo-fect solution (System Biosciences), and then incubated at 37°C for 10 min. To stop the reaction, the transfected exosomes were mixed with 30 μl ExoQuick-TC (System Biosciences) and incubated at 4°C for 30 min. After centrifugation of samples for 3 min at 14,000 rpm, the transfected exosomes were suspended in PBS.

Western blotting. Cells were lysed in lysis buffer (Roche, Mannheim, Germany), and equal amounts of protein were separated on sodium dodecyl sulfate-polyacrylamide gels. The exosomal pellets isolated from equal volumes of culture medium (5 ml) were lysed in 200 μl of lysis buffer. Equal volumes of lysate (30 μl) were loaded in the lanes and western blots were

probed with antibodies directed against αSMA (rabbit polyclonal anti-αSMA; 1:500; C-28; Santa Cruz Biotechnology, Santa Cruz, CA, USA), β-actin (mouse monoclonal anti-β-actin; 1:2500; Chemicon, Temecula, CA, USA), CD63 (mouse monoclonal anti-CD63; 1:100; sc-5275; Santa Cruz), CD81 (mouse monoclonal anti-CD81; 1:100; sc-23962; Santa Cruz), and TSG101 (mouse monoclonal anti-TSG101; 1:100; ab83; Abcam, Cambridge, United Kingdom) as EV markers. Horseradish peroxidase-conjugated secondary antibodies were purchased from GE Healthcare (Milwaukee, WI, USA).

***In vivo* evaluation of a novel porous 3D scaffold.** BMSCs were incubated in MSCGM medium containing NEO-STEM TSR50 (RITC; 0.1 mg/ml, Biterials, Seoul, Korea) overnight at 37°C in 5% CO_2, followed by incubation in MSCGM medium for 6 h and washing in PBS before injection into the scaffold. NEO-STEM labeling of BMSCs was confirmed by fluorescence microscopy (Biozero BZ-8000; Keyence). To visualize MM cells in a 3D porous scaffold, MM cell lines (RPMI 8226, KMS-11, U266) were transduced with a lentiviral vector expressing firefly luciferase and GFP (BLIV713PA-1; System Biosciences, Mountain View, CA, USA). After selection with puromycin, drug-resistant and GFP+ cells were analyzed 10 days after

infection.Hydroxylapatite (HA)-based 3D porous scaffolds (GC Corporation, Tokyo, Japan) were immersed in 35 μl of culture medium with NEO-STEM-labeled BMSCs (5×10^5 cells/scaffold) and GFP-overexpressed MM cell lines (RPMI 8226-GFP, KMS-11-GFP, or U266-GFP, 5×10^5 cells per scaffold). The scaffolds were impregnated with cells by capillary action by placing them on Whatman 3MM filter paper and creating a vacuum. The scaffolds were left to rest for 5 min after impregnation and were then incubated at 37°C for 24 h, before subcutaneous implantation into nude mice (female, 8-week-old BALB/c-n/n; CLEA Japan, Tokyo, Japan). All experimental groups included three mice.

Isolation of CD138+ myeloma cells derived from MM patients. Bone marrow mononuclear cells were isolated by Ficoll-Conray (Lymphosepar I, Immuno-Biological Laboratories Co., Gunma, Japan) and sorted into two fractions containing CD138+ and CD138− cells, respectively, using CD138 Microbeads (Miltenyi Biotec, Bergisch Gladbach, Germany) and an Auto-MACS Pro (Miltenyi Biotec), according to the manufacturer's instructions. CD138+ cells sorted from four MM patients were cultured in serum-free AIM-V medium (Invitrogen, Carlsbad, CA, USA). After 24 h of incubation, EVs were isolated from each culture medium

using Exoquick-TC (System Biosciences, Mountain View, CA, USA). The spike-in synthetic miRNA (ath-miR-159) was used as an invariant control for EV miRNA.

SUPPLEMENTARY FIGURES

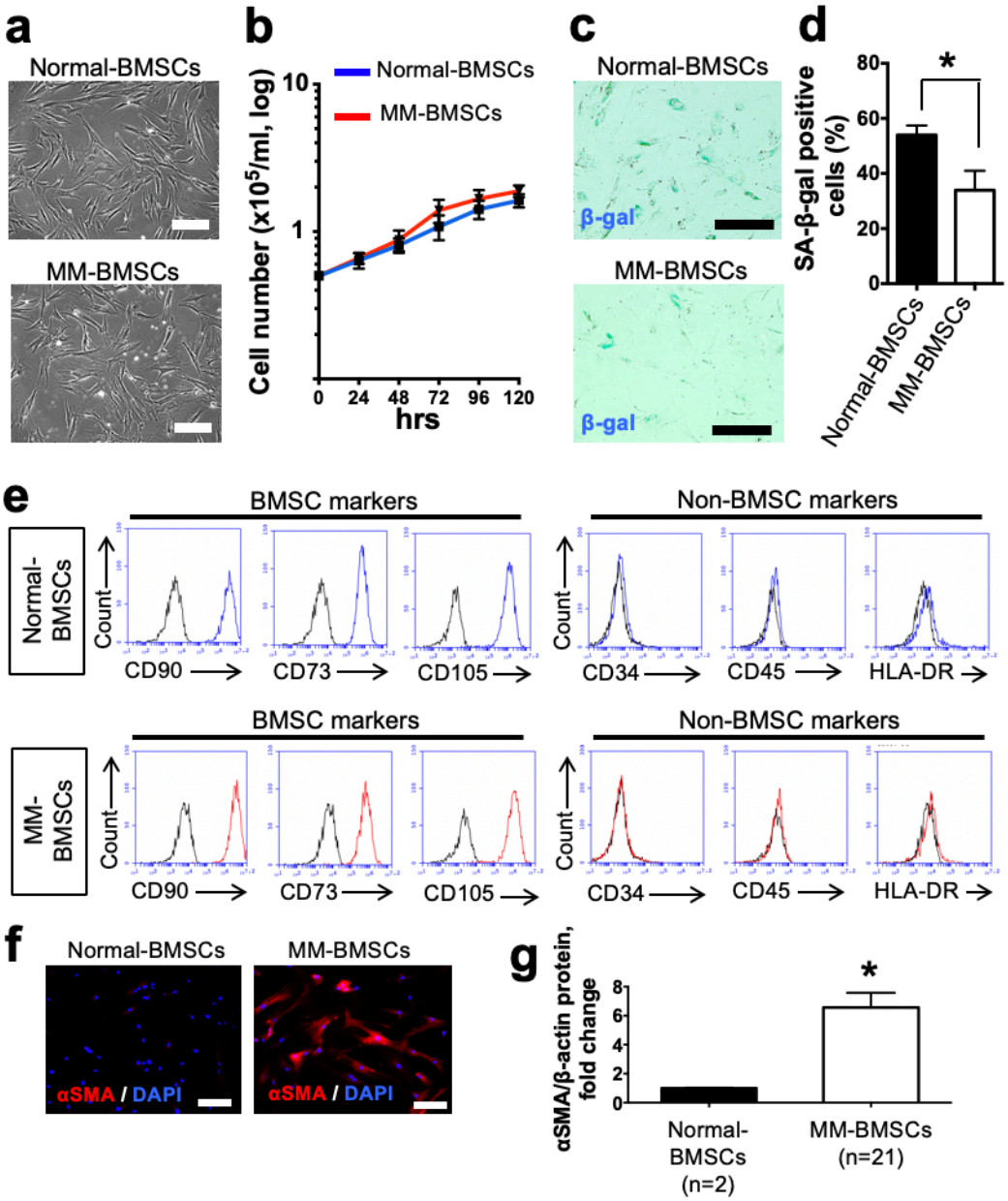

Supplementary Fig. 1 (Umezu et al.)

Supplementary Figure 1. Phenotypic markers of cancer-associated fibroblasts (CAFs) were increased in BMSCs derived from MM patients. (a) Representative morphology of BMSCs derived from healthy donors (Normal-BMSCs) and patients with MM (MM-BMSCs) by phase-contrast inverted microscopy. There were no differences in morphology or proliferation rate between MM-BMSCs and BMSCs from age-matched healthy donors (Normal-BMSCs). Scale bar, 50 μm. (b) Growth of BMSCs was measured after 24, 48, 72, 96, and 120 h. Proliferation of Normal-BMSCs (n = 2, blue line) and MM-BMSCs (n = 6, red line). Values represent the mean ± S.D. There was no significant difference in proliferation rate between Normal-BMSCs and MM-BMSCs by 120 h in culture. (c) Representative SA-β-gal staining images (arrows indicate SA-β-gal+ cells) and quantification of cell senescence. Scale bar, 50 μm. (d) SA-β-gal staining results (mean ± S.D). *P < 0.01 compared with Normal-BMSCs (Student's t-test). However, MM-BMSCs included significantly fewer senescence-associated beta-galactosidase (SA-β-gal)-positive cells than Normal-BMSCs at the same passage ($P < 0.01$). (e) BMSC phenotype determined by immunohistochemical staining of cell surface markers (CD90+, CD73+, CD105+, CD34−, CD45−, HLA-DR−) by flow cytometry, thereby demonstrating an immunophenotype characteristic of human mesenchymal

stromal cells. Black histograms indicate background staining with isotype controls, and red and blue histograms indicate frequencies of cells stained with markers. (f) Immunofluorescence of αSMA in Normal-BMSC s and MM-BMSCs. Staining was representative of experiments performed using two different Normal-BMSC samples and six different MM-BMSC samples. MM-BMSCs also showed significantly more cells positive for the active cancer-associated fibroblast (CAF) marker, α-smooth muscle actin (αSMA), compared with Normal-BMSCs. Scale bar, 25 μm. (g) Western blot analysis of αSMA protein expression in Normal-BMSCs (n = 2) and MM-BMSCs (n = 21). Densitometric analysis comparing relative expression level of αSMA normalized to β-actin expression. Western blot analysis confirmed αSMA expression levels were significantly increased in MM-BMSCs compared with Normal BMSCs ($P < 0.01$).

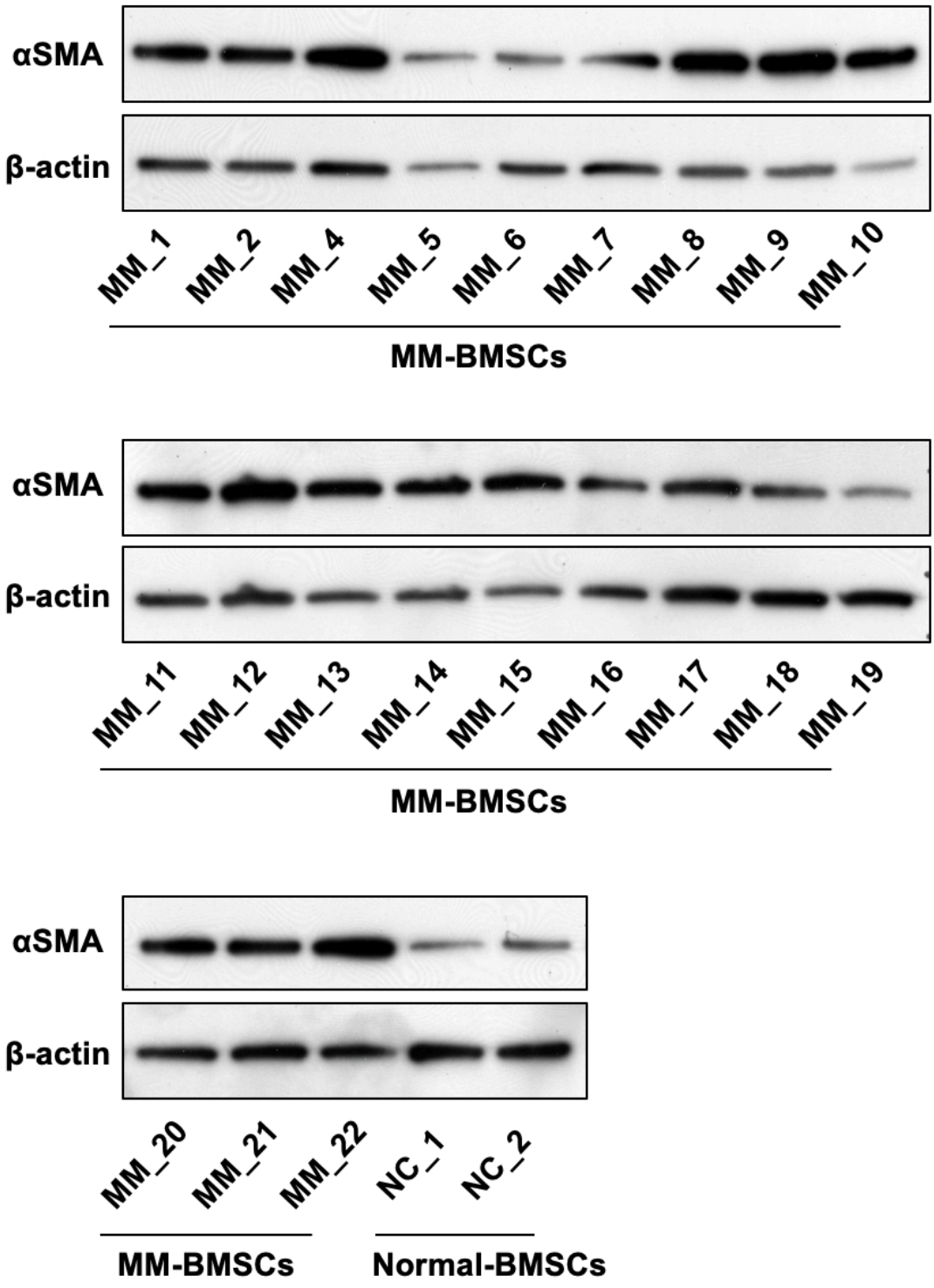

Supplementary Fig. 2 (Umezu et al.)

Supplementary Figure 2. Characterization of BMSCs. Western blot analysis of alpha-smooth muscle actin (αSMA) and β-actin protein expression in Normal-BMSCs (n = 2) and MM-BMSCs (n = 21).

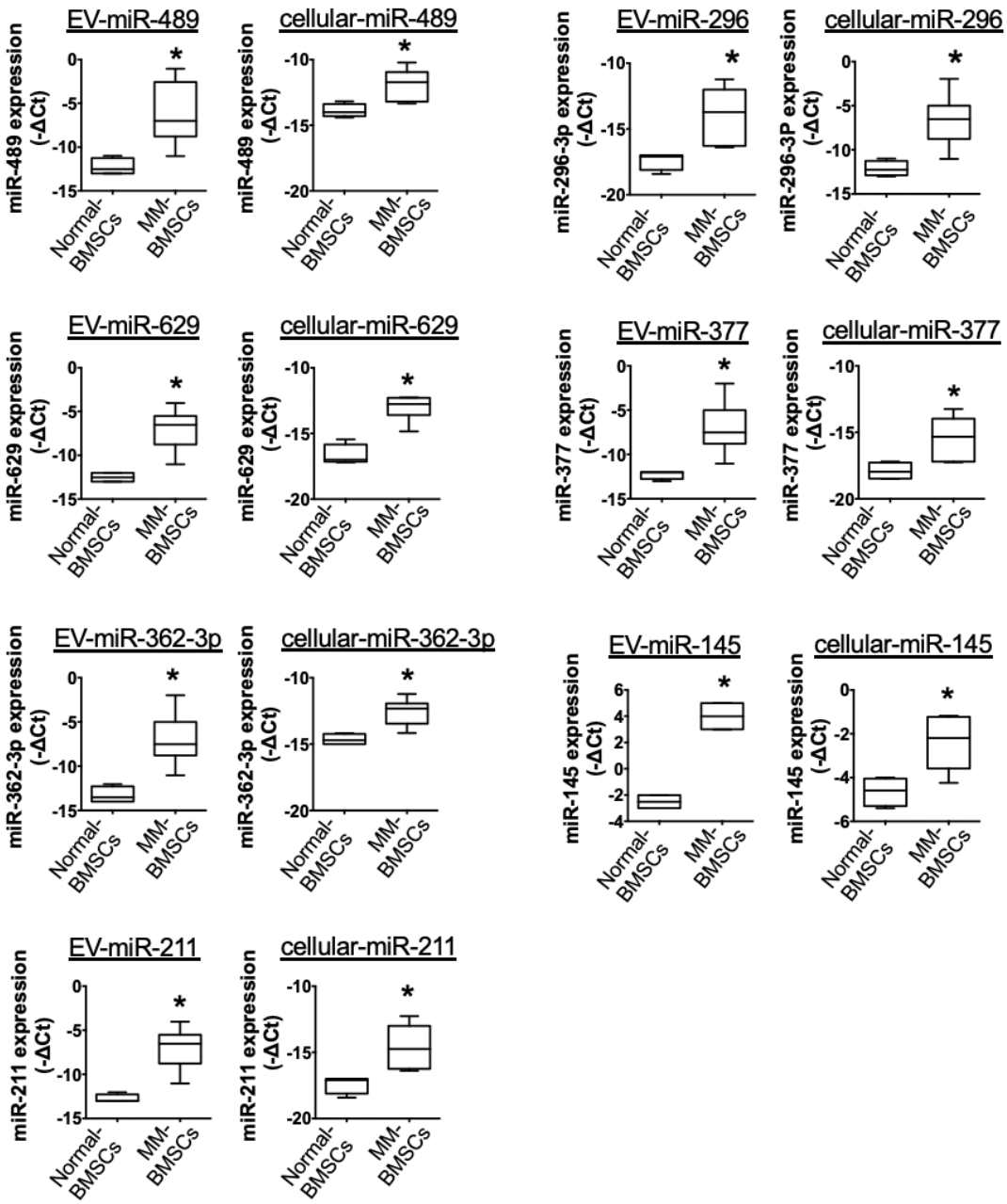

Supplementary Fig. 3 (Umezu et al.)

Supplementary Figure 3. Differential miRNA expression in EVs derived from Normal-BMSCs and MM-BMSCs. Expression levels of EV and cellular miRNAs (miR-489, miR-629, miR-362-3p, miR-211, miR-296, miR-377, and miR-145) in Normal-BMSCs and MM-BMSCs by TaqMan Low Density Array (TLDA) array. Box plot whiskers represent minimum and maximum values and P values were calculated using independent-samples *t*-tests. *$P < 0.01$.

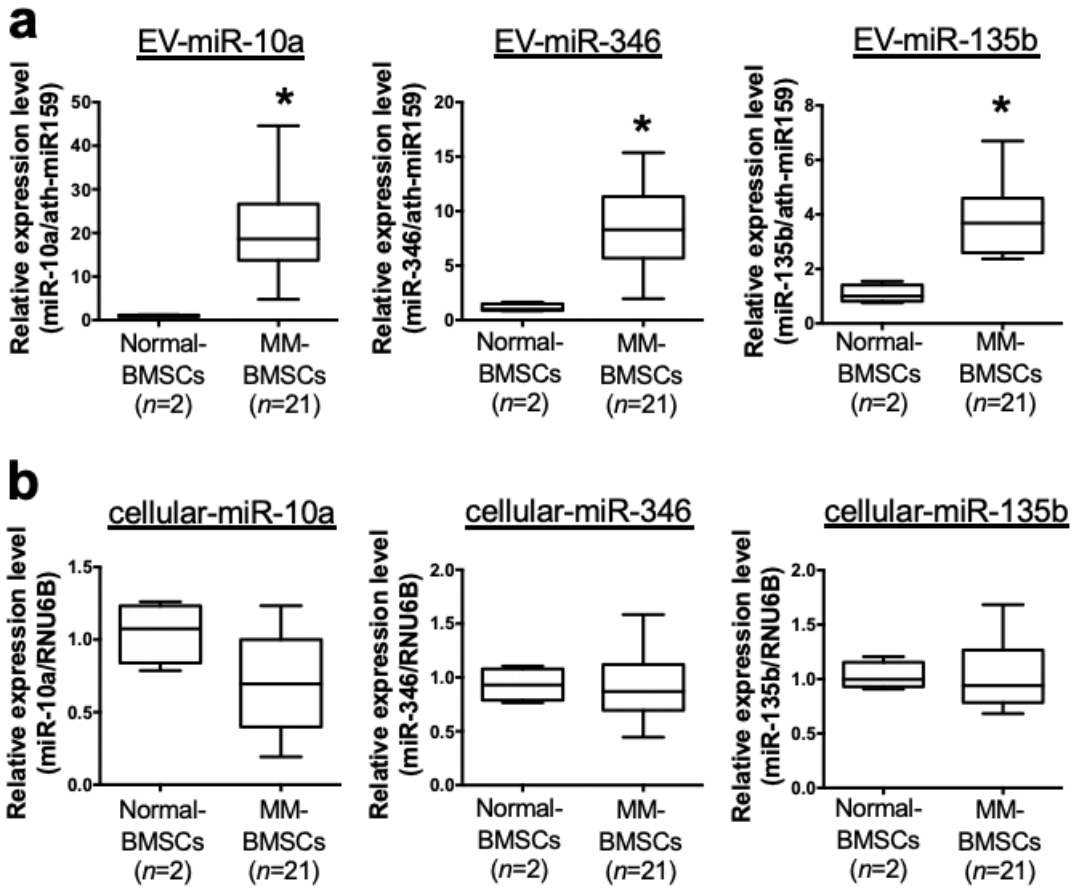

Supplementary Fig. 4 (Umezu et al.)

Supplementary Figure 4. Intercellular and EV miRNA expression levels in Normal-BMSCs and MM-BMSCs. To confirm the results of TaqMan miRNA arrays, we quantified cellular miRNA (a) and EV miRNA (b) (miR-10a, miR-346, and miR-135b) expression levels in Normal-BMSCs (n = 2) and MM-BMSCs (n = 6) by qRT-PCR. Box plot whiskers represent minimum and maximum values and P values were calculated using independent-samples *t*-tests. *P < 0.01.

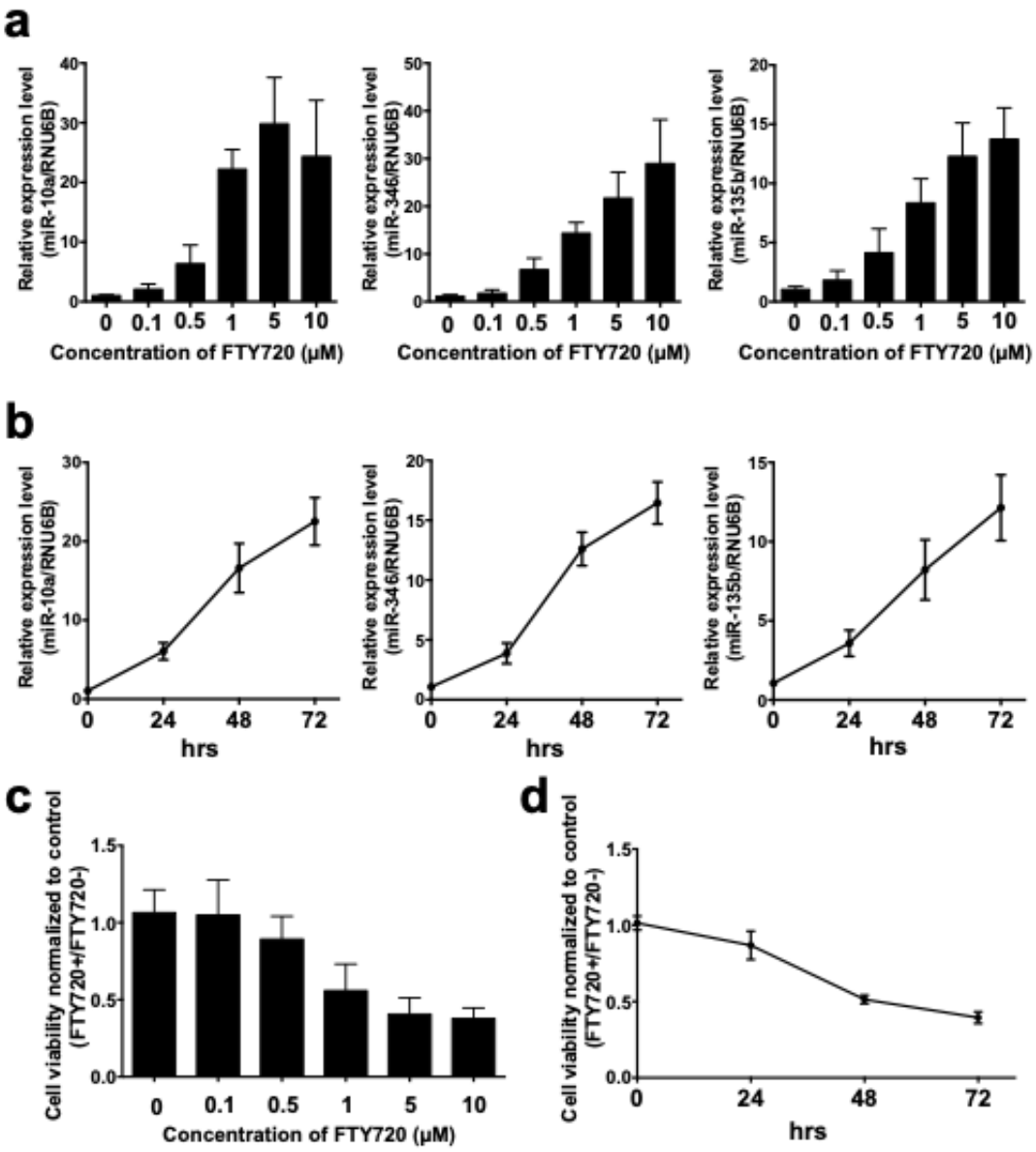

Supplementary Fig. 5 (Umezu et al.)

Supplementary Figure 5. Dose- and time-dependent accumulation of cellular miR-10a,

miR-346, and miR-135b induced by FTY720. (a,b) qRT-PCR analysis of cellular miR-10a, miR-346, and miR-135b expression in MM-BMSCs (n = 6) treated with increasing concentrations of FTY720 for 48 h (a); time course of miR-10a expression following treatment with 1 μM FTY720 for 0–96 h (b). Dose- and time-dependent accumulation of cellular miR-10a, miR-346, and miR-135b were observed after FYT720 exposure in MM-BMSCs. (c) Cell viability was measured in MM-BMSCs (n = 6) following 48 h of treatment with increasing concentrations of FTY720, using a Cell Counting Kit-8. (d) Time course of viability of MM-BMSCs (n = 6) treated with 1 μM FTY720. Data represent fold increase compared with control (without FTY720) ± S.D. Dose- and time-dependent inhibition of viability of MM-BMSCs was observed after FYT720 exposure.

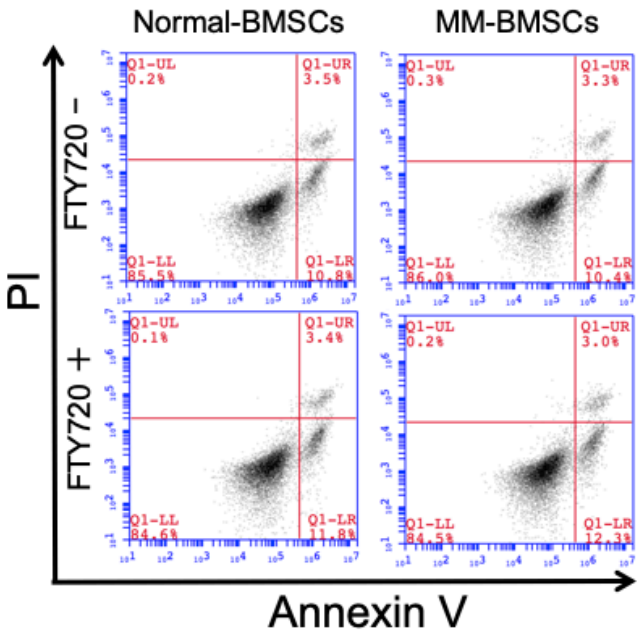

Supplementary Fig. 6 (Umezu et al.)

Supplementary Figure 6. Apoptosis of Normal-BMSCs was unaffected by treatment with FTY720 for 24 h. Normal-BMSCs and MM-BMSCs were treated with 1 μM FTY720 and apoptosis rates were determined after 24 h, using Annexin V and PI staining and flow cytometry.

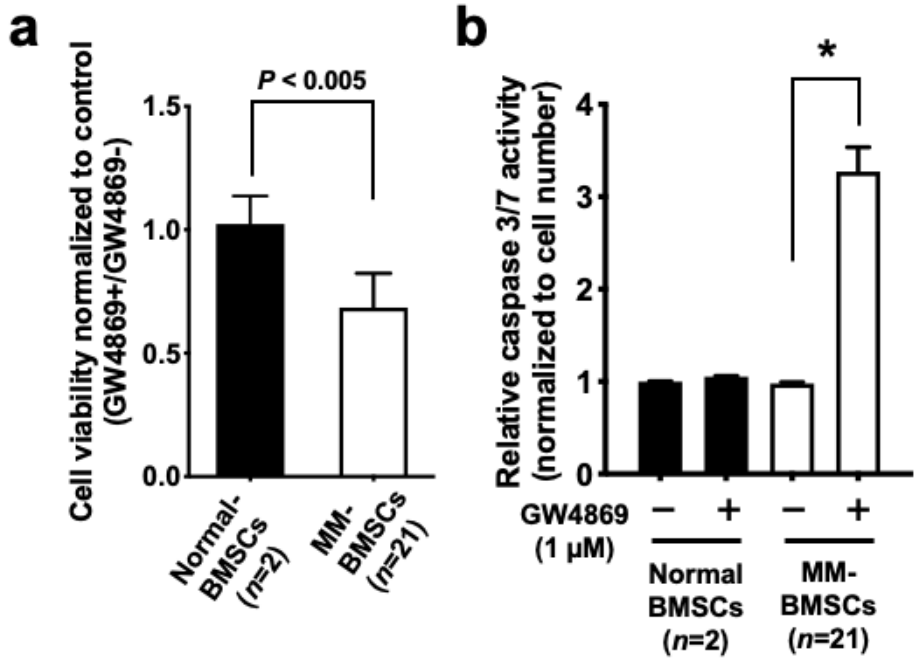

Supplementary Fig. 7 (Umezu et al.)

Supplementary Figure 7. GW4869 inhibited cell growth and induced apoptosis in MM-BMSCs. Normal-BMSCs (n = 2) and MM-BMSCs (n = 21) were cultured with or without GW4869 (5 μM). (a) Cell viability after 48 h. Values represent growth rate normalized by control (GW4869+/GW4869-) ± S.D. GW4869 reduced the viability of MM-BMSCs (n = 21)

but not Normal-BMSCs ($P < 0.005$) as well as FTY740 (Figure 3a). (b) Caspase-3/7 activity measured after 48 h. Data represent fold increase compared with control (without GW4869) ± S.D. Caspase 3/7expression levels increased significantly in MM-BMSCs treated with 5 μM GW4869 compared with untreated cells ($P < 0.01$), while no similar effect was observed in Normal-BMSCs.

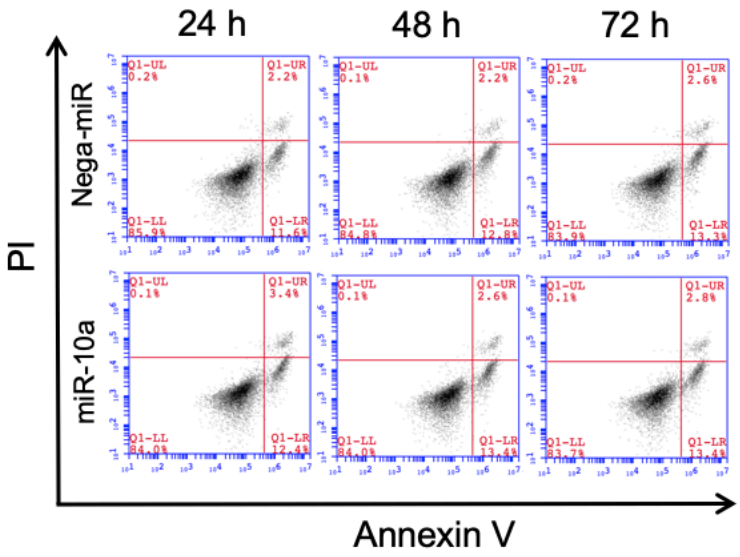

Supplementary Fig. 8 (Umezu et al.)

Supplementary Figure 8. Apoptosis of Normal-BMSCs was unaffected by miR-10a overexpression for 24–72 h. Time-course of apoptosis induced by miR-10a transfection in Normal-BMSCs, determined by Annexin V and PI staining and flow cytometry.

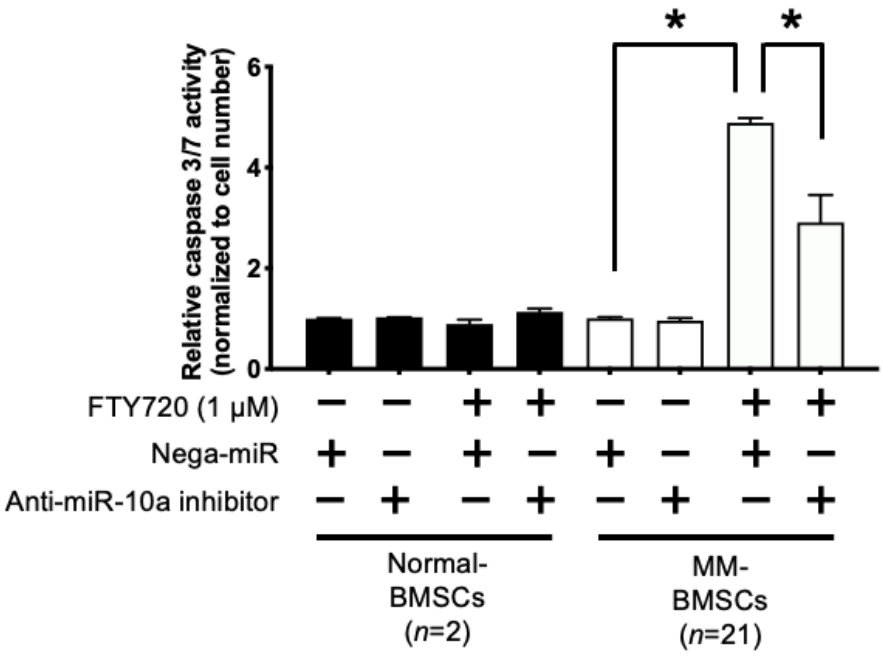

Supplementary Fig. 9 (Umezu et al.)

Supplementary Figure 9. Apoptosis induction by FTY720 inhibiting EVs release and accumulating miR-10a in the BMSCs. Normal-BMSCs (*n* = 2) and MM-BMSCs (*n* = 21) transfected with 10 nM Negative control-miR (Nega-miR) or 10 nM anti-*miR-10a* inhibitor were cultured with or without FTY720 (1 μM). Caspase-3/7 activity measured after 48 h. Data represent fold increase compared with control (Nega-miR-transfected Normal-BMSCs without

FTY720) ± S.D. Induction of apoptosis in MM-BMSCs treated with FTY720 was canceled by transfection of anti-miR-10a inhibitor (*$P < 0.01$).

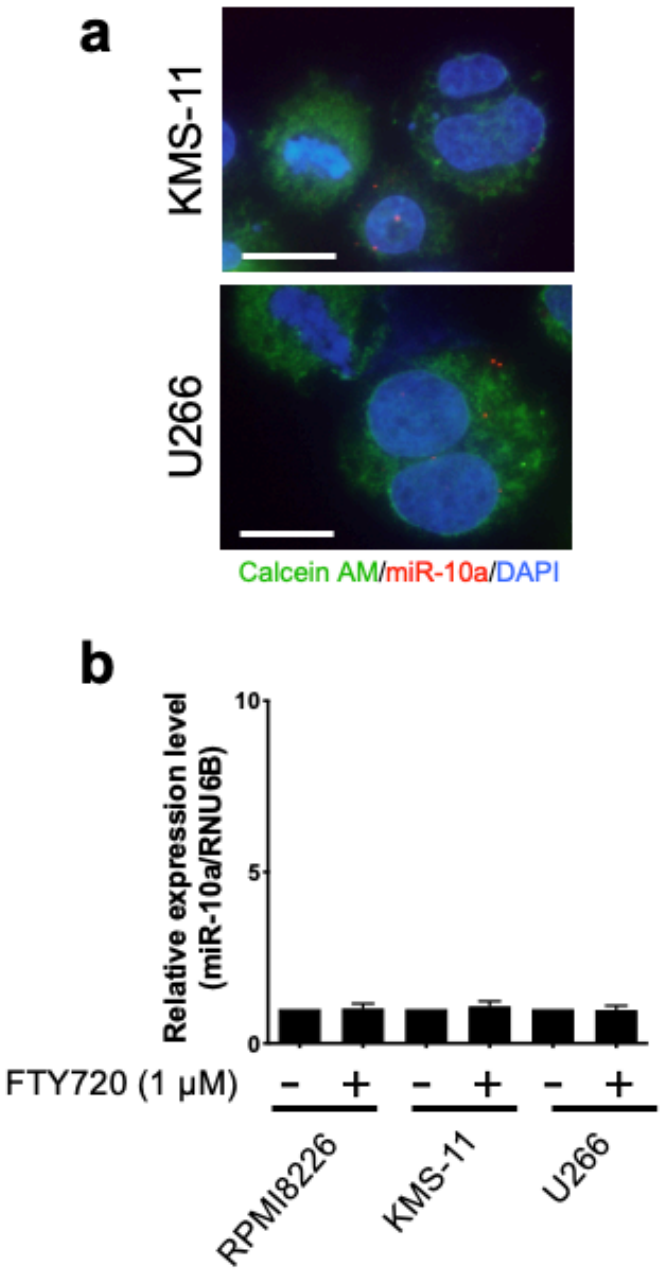

Supplementary Fig. 10 (Umezu et al.)

Supplementary Figure 10. EV miR-10a derived from MM-BMSCs transferred to KMS-11 and U266. (a) KMS-11 and U266 treated with EVs directly transfected with Cy3-miR-10a mimics for 48 h, and noted dots indicating Cy3-miR-10a in the cytoplasm. Nuclear and cytoplasmic staining with DAPI (blue) and calcein AM (green), respectively. Scale bar, 20 μm. (b) Expression levels of *miR-10a* in RPMI 8226, KMS-11, and U266 MM cells treated with 1 μM FTY720 for 48 h, measured by qRT-PCR. Data represent fold increase compared with control (without FTY720) ± S.D.

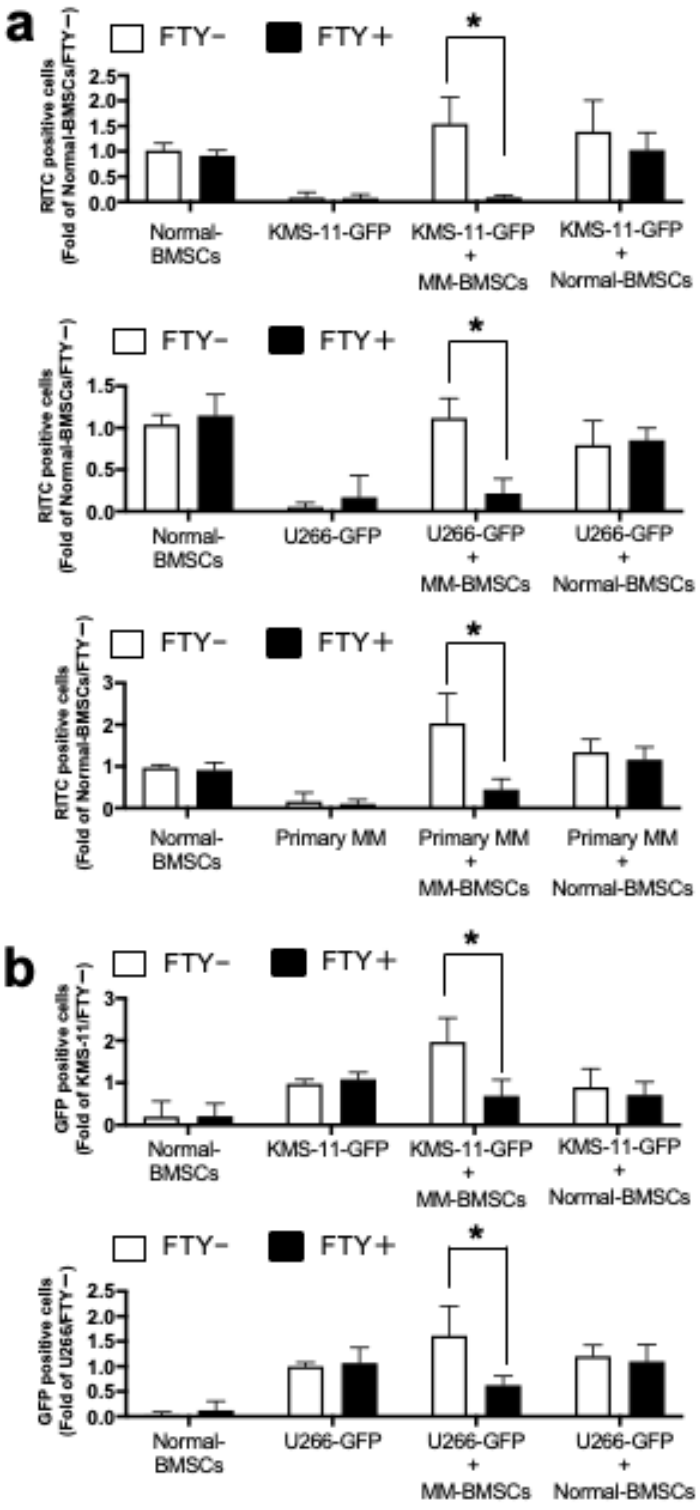

Supplementary Fig. 11 (Umezu et al.)

Supplementary Figure 11. FTY720 indirectly and directly inhibited the proliferation of MM cells *in vivo*. Fluorescence microscopic examination of RITC+ cells (nanoparticle-labeled BMSCs) and GFP+ cells (KMS-11-GFP, U266-GFP) 8 weeks after implantation of scaffolds impregnated with Normal-BMSCs, MM cell lines or primary MM cells,, MM cells + MM-BMSCs, and MM cells + Normal-BMSCs. (a) Quantitative data for RITC+ cells in the scaffold determined by pixel density. $*P < 0.01$ (Student's *t*-test). Values are mean ± SD. (b) Quantitative data for GFP+ cells in the scaffold determined by pixel density. $*P < 0.01$ (Student's *t*-test). Values are mean ± SD. FTY+, mice treated with 1 mg/kg FTY720; FTY−, mice without FTY720.

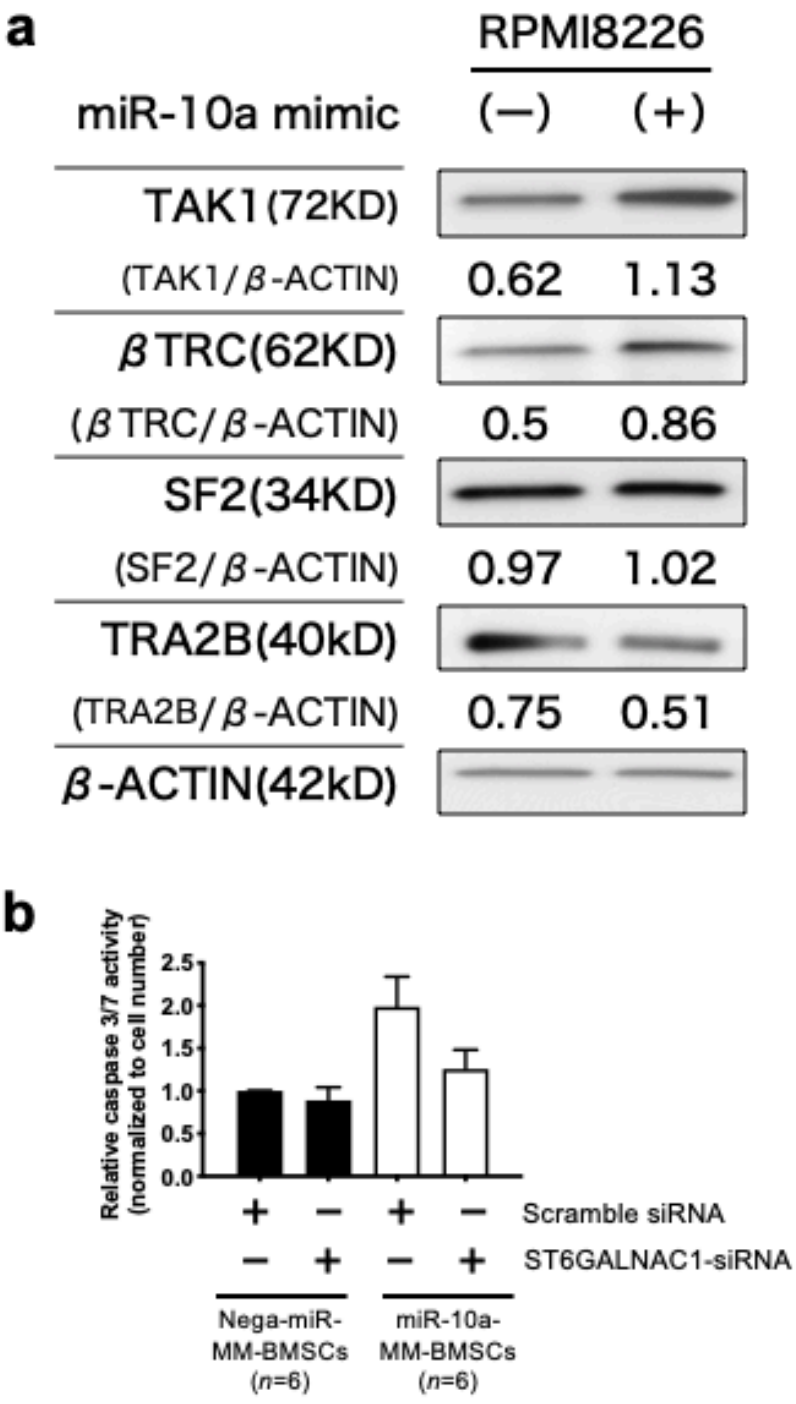

Supplementary Fig. 12 (Umezu et al.)

Supplementary Figure 12. Direct target genes of *miR-10a* in MM cells and MM-BMSCs.

(a) We searched miRTarBase and TargetScan for direct target genes of *miR-10a* in MM cells. From the search results, we extracted four candidate genes including *TAK1*. The expression of candidate *miR-10a* target factors in MM cells overexpressing *miR-10a* was analyzed by western blotting. Of the four factors analyzed, SF2 and TRA2B expression was not significantly different, but interestingly, TAK1 and βTRC expression was elevated by *miR-10a* overexpression. Although not affected by the TAK1 inhibitor, treatment with βTRC inhibitor canceled the promotion of cell proliferation by *miR-10a* overexpression in MM cells.

(b) We searched for direct target genes of *miR-10a* in MM-BMSCs using TargetScan. Among the genes whose expression was decreased in MM-BMSCs by *miR-10a* overexpression, we extracted candidate genes with conserved *miR-10a* binding sites. Furthermore, we found that *ST6GALNAC1* was specifically expressed in MM-BMSCs compared with Normal-BMSCs among the candidate genes. *ST6GALNAC1*. Apoptosis induction by overexpression of *miR-10a* in MM-BMSCs was attenuated by knockdown of *ST6GALNAC1* by siRNA.

Supplementary table 1. DAVID functional annotation analysis of the 228 genes downregulated by miR-10a overexpression in MM-BMSCs

GO term	Gene count	Genes	*p*-value
GO:0008283 cell proliferation	43	CCL2, PODN, CYP1B1, TBC1D8, PRC1, CD248, SDC4, PTEN, CXCL12, FAM83D, ANXA7, SPINT2, GMNC, PER2, RC3H2, PTN, CD4	4.58173E-05
GO:0010941 regulation of cell death	35	IER3IP1, HTATIP2, CCL2, THRA, CYP1B1, GRIK2, LGMN, CD248, TLR3, PTEN, CXCL12, PTGIS, WISP1, COMP, PTN, NQO1, TWIST2	0.000284898
GO:0001666 response to hypoxia	13	MUC1, ICAM1, BMP2, PTGIS, CCL2, EPAS1, MDM2, PTN, CYGB, CXCL12, PTEN, NDNF, DDIT4	0.000194925
GO:0030334 regulation of cell migration	22	ICAM1, RAP2A, IL6, BMP2, CCL2, CYP1B1, PODN, TGFBR1, COL3A1, HGF, SDC4, PTEN, CXCL12, FBLN1, MEOX2, KIF20B, SEMA3C	8.80405E-05
GO:0001649 osteoblast differentiation	12	BMP2, IL6, ID1, FAM20C, H3F3B, CDK6, ID3, HGF, IGFBP3, TPM4, TWIST2, IGFBP5	2.58319E-05
GO:0042493 response to drug	18	ABCA8, ICAM1, RAP2A, IL6, CCL2, ACER2, NUDT15, TLR3, CPS1, SLC47A1, PTEN, CPT1A, TFRC, FABP3, PTN, MDM2, SEMA3C, WFDC1	1.08644E-05

Supplementary table 2. DAVID functional annotation analysis of the 50 genes downregulated by miR-10a overexpression in MM cells

GO term	Gene count	Genes	*p*-value
GO:0008283 cell proliferation	7	NAMPT, PTGES, CCR3, SMAD4, DMRT1, XCL1, PRKX	0.01072711
GO:0050896 response to stimulus	22	IGLV1-40, OR2L8, NAMPT, GATSL2, SNRPN, RRH, SMAD4, DMRT1, APOLD1, PDE3B, GSTT1, GTF2H2, TAS2R46, CSNK1E, PTGES, SLC25A23, HSP90AB4P, CCR3, IGHA1, XCL1, SLC22A1, KIR3DL2	0.015439828
GO:0034762 regulation of transmenbrane transport	4	CALHM1, KCND1, KCNJ10, XCL1	0.032204358
GO:0001525 angiogenesis	4	CCR3, APOLD1, PDE3B, PRKX	0.03363268
GO:0019724 B cell mediated immunity	3	IGLV1-40, IGHA1, XCL1	0.035718174